HOLOGIC®
The Science of Sure

Powerful images.
Clear answers.

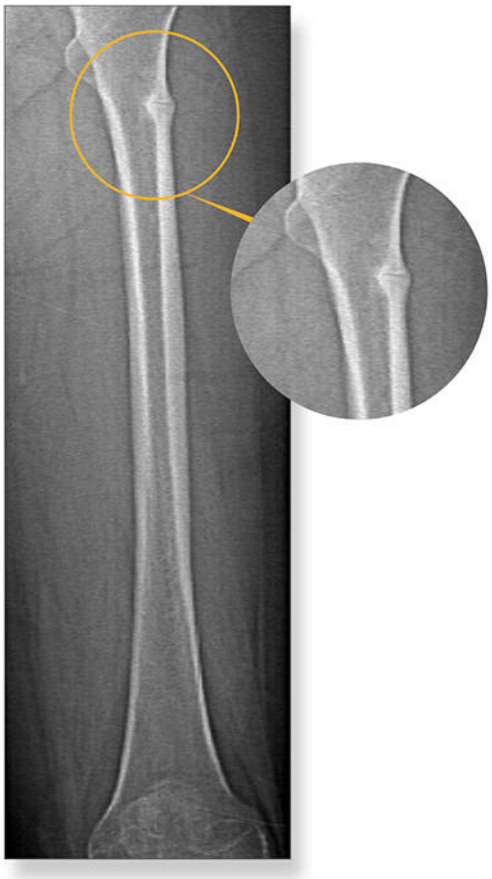

Manage Patient's concerns about Atypical Femur Fracture*

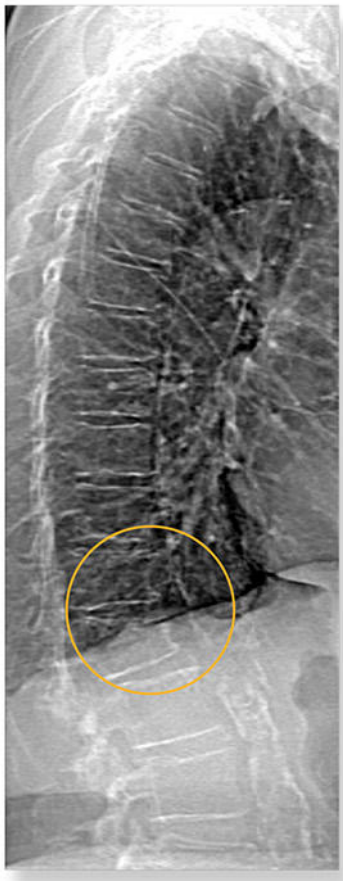

Vertebral Fracture Assessment – a critical part of a complete fracture risk assessment

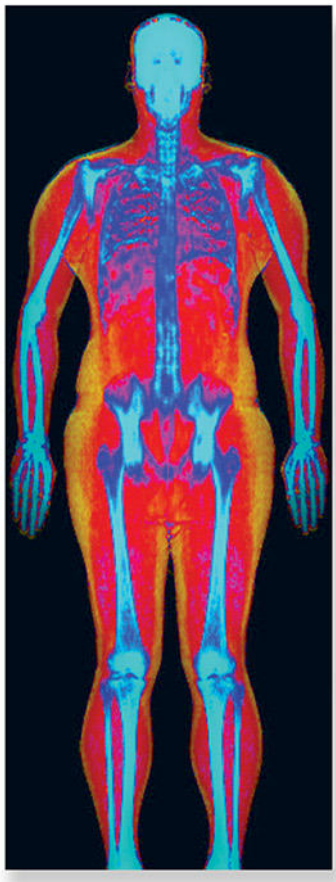

Advanced Body Composition® Assessment – the power to see what's inside

Contact your Hologic rep today at insidesales@hologic.com

*Incomplete Atypical Femur Fractures imaged with a Hologic densitometer, courtesy of Prof. Cheung, University of Toronto

www.hologic.com | info@hologic.com | 1.781.999.7300

Original Article

Androgen Receptor in Neurons Slows Age-Related Cortical Thinning in Male Mice†

Ferran Jardí,[1] Nari Kim,[1] Michaël R. Laurent,[2,3] Rougin Khalil,[1] Ludo Deboel,[1] Dieter Schollaert,[1] Harry van Lenthe, [4] Brigitte Decallonne,[1] Geert Carmeliet,[1] Frank Claessens,[2] and Dirk Vanderschueren[1]

[1] Clinical and Experimental Endocrinology, Department of Chronic Diseases, Metabolism and Aging (CHROMETA), KU Leuven, Herestraat 49 PO box 902, 3000 Leuven, Belgium

[2] Molecular Endocrinology Laboratory, Department of Cellular and Molecular Medicine, KU Leuven, Herestraat 49 PO box 901, 3000 Leuven, Belgium

[3] Gerontology and Geriatrics, Department of Chronic Diseases, Metabolism and Aging (CHROMETA), KU Leuven, Herestraat 49 PO box 7003, 3000 Leuven, Belgium

[4] Biomechanics Section, Department of Mechanical Engineering, KU Leuven, Leuven, Belgium

Corresponding author:

Prof. dr. Dirk Vanderschueren

Clinical and Experimental Endocrinology, KU Leuven

Herestraat 49 PO box 902

3000 Leuven, Belgium

tel. +32 16 3 46987

dirk.vanderschueren@uzleuven.be

2 supplemental tables and 3 supplemental figures have been included with the submission.

†This article has been accepted for publication and undergone full peer review but has not been through the copyediting, typesetting, pagination and proofreading process, which may lead to differences between this version and the Version of Record. Please cite this article as doi: [10.1002/jbmr.3625]

Additional Supporting Information may be found in the online version of this article.

Initial Date Submitted July 2, 2018; Date Revision Submitted October 30, 2018; Date Final Disposition Set November 5, 2018

Journal of Bone and Mineral Research

DOI 10.1002/jbmr.3625

Funding:

Research Foundation Flanders (FWO) [grant G0D2217N]
KU Leuven Research Council [grant GOA/15/017]
FJ is supported by a post-doctoral grant from FWO.

Disclosures:

All authors state that they have no conflicts of interest.
This work was selected for oral presentation both at the 2017 American Society for Bone and Mineral Research (ASBMR) Scientific Meeting, being included in its Annual Meeting Highlights Session, and at the 2018 European Calcified Tissue Society (ECTS) Congress.
Ferran Jardí received the 2017 ASBMR Young Investigator Award for this work.

Abstract

Androgens via the androgen receptor (AR) are required for optimal male bone health. The target cell(s) for the effects of androgens on cortical bone remain(s) incompletely understood. In females, estrogen receptor alpha in neurons is a negative regulator of cortical and trabecular bone. Whether neuronal AR regulates bone mass in males remains unexplored. Here, we inactivated AR in neurons using a tamoxifen-inducible CreERT2 under the control of the neuronal promoter Thy1. Tamoxifen induced a 70-80% reduction of AR mRNA levels in Thy1-CreERT2 positive brain regions cerebral cortex and brainstem as well as in the peripheral nervous tissue of male neuronal AR knockout (N-ARKO) mice. Hypothalamic AR mRNA levels were only marginally reduced and the hypothalamic-pituitary-gonadal axis remained unaffected, as determined by normal levels of serum testosterone, LH and FSH. In contrast to orchidectomy, deletion of neuronal AR did not alter body weight, body composition, hindlimb muscle mass, grip strength or wheel running. MicroCT analysis of the femur revealed no changes in bone accrual during growth in N-ARKO mice. However, 36- and 46-week-old N-ARKO mice displayed an accelerated age-related cortical involution, namely a more pronounced loss of cortical thickness and strength, which occurred in the setting of androgen sufficiency. Neuronal AR inactivation decreased the cancellous bone volume fraction in L5 vertebra but not in the appendicular skeleton of aging mice. MicroCT findings were corroborated in the tibia and after normalization of hormonal levels. Serum markers of bone turnover and histomorphometry parameters were comparable between genotypes, except for a 30% increase in osteoclast surface in the trabecular compartment of 36-week-old N-ARKO mice. Cortical bone loss in N-ARKO mice was associated with an up-regulation of *Ucp1* expression in brown adipose tissue, a widely used readout for sympathetic tone. We conclude that androgens preserve cortical integrity in aging male mice via AR in neurons.

Keywords: aging, bone-brain-nervous system interactions, genetic animal models, neuroendocrine and sex steroids

This article is protected by copyright. All rights reserved

Androgens are crucial regulators of skeletal health in males [1]. Male hypogonadism is a well-established cause of decreased BMD in both humans and rodents whilst testosterone (T) replacement normalizes and maintains BMD [2,3]. Although several effects of T on bone result from aromatization to estradiol (E2) and subsequent activation of estrogen receptor alpha (ERα), it is now clear from studies in transgenic mice that androgens also act directly on the androgen receptor (AR) to stimulate bone mass [4]. In particular, AR activation in osteoblasts inhibits bone resorption in the cancellous compartment [5,6]. However, the cellular targets mediating the well-established effects of T on cortical bone formation and maintenance remain elusive. Neither osteoblast- nor osteoclast-lineage conditional deletions of AR impair cortical mass in male mice [5–7], suggesting that androgens act on other target cells outside bone to stimulate periosteal bone formation.

Bone mass starts declining progressively in men during the third decade of life, before any decay in sex steroid levels, and continues at a constant relative rate until accelerating around 75 years of life [8]. In elderly men, low androgens and estrogens concentrations have been associated with higher rates of BMD loss [4], suggesting a role for sex steroids slowing the age-associated bone involution in men. The onset of bone loss in male rodents also occurs during early adulthood but, unlike men, their androgen bioactivity levels remain stable with aging [9]. Nevertheless, AR actions might still be important for post-pubertal bone health in male mice [6,10], even when mechanisms other than sex steroid deficiency drive age-related bone loss in rodents.

The central nervous system (CNS) participates actively, along with autocrine, paracrine and endocrine factors, in bone mass control. The first evidence of a central regulation of bone mass was provided by Karsenty's group, showing that intracerebroventricular infusion of leptin completely reversed the high bone mass phenotype of *ob/ob* mice [11,12]. Similarly, in female rodents, normal skeletal mass is determined by the balance between peripheral stimulatory and central inhibitory actions of ERα [13,14]. Also in female rodents, an increase in the sympathetic nervous system (SNS) outflow appears to mediate, at least in part, the bone loss resulting from ovariectomy (OVX). In particular, treatment with β-adrenergic receptor blockers prevents trabecular deterioration in OVX rats [15]. Moreover, female

mice with a genetic deletion of beta 2 adrenergic receptor (*Adrb2*) are protected from bone resorption after estrogen depletion [16]. Since sympathetic projections in bone are located in close vicinity to osteoblasts and are anatomically linked to the CNS [12,17], it is conceivable that the SNS acts as a downstream mechanism through which central ERα inhibits bone formation in females.

Despite the substantial amount of evidence showing that estrogen actions on the CNS determine bone mass in females, similar data supporting a central component in AR regulation of male skeleton are not available. We hypothesized that androgen signaling through AR expressed in neurons would mediate, at least partly, the effects of AR on cortical acquisition and/or contribute to maintain post-pubertal cortical health in male mice. To this end, we generated and characterized mice with AR deletion in neurons and analyzed their cortical and trabecular phenotype both at peak bone mass and in aging. This neuronal ARKO (N-ARKO) mouse line targets AR actions outside the hypothalamus and thereby avoids potential confounding effects induced by AR hypothalamic insensitivity and altered negative feedback in the hypothalamic-pituitary-gonadal (HPG) axis. Our findings show for the first time that AR in neurons maintains bone mass and strength in aging mice by restraining bone resorption and the consequent cortical thinning associated with aging.

Materials and Methods

Study design

All experiments involving animals were conducted with approval of the KU Leuven ethical committee (P041/2014). Mice with a neuronal-specific knockout of the AR (N-ARKO) neurons were generated as previously described [18] and maintained on a C57Bl/6J background. Thy1-CreERT2 transgenic mice display a high recombination efficiency in projecting neurons in both the peripheral and central nervous systems, except for the hypothalamus, caudate putamen, ventral striatum and basal forebrain [19]. Noteworthy, hypothalamic neurons could be indirectly affected through nerve projections from other brain areas. Male mice expressing Thy1-CreERT2 were crossed with female mice carrying a heterozygous floxed exon 2 of the AR [20]. At 6 weeks of age, both male N-ARKO ($AR^{fl/Y}$; Thy-$CreERT2^{+/-}$) and their wild-type ($AR^{+/Y}$), hemizygous exon 2 floxed ($AR^{fl/Y}$) and hemizygous Thy1-

CreERT2 ($AR^{+/Y}$; Thy-$CreERT2^{+/-}$) control littermates were gavaged with tamoxifen (190 mg/kg body weight; Sigma-Aldrich) once daily for 2 consecutive days. This shortened tamoxifen protocol has been described previously to efficiently induce CreER-mediated gene deletion in male mice without off-target effects on bone [18]. A group of $AR^{fl/Y}$; Thy-CreERT2 mice were gavaged with vehicle (ethanol: sunflower seed oil; 1:9) to control for potential tamoxifen-independent CreERT2 activity. Animals were euthanized by pentobarbital anesthesia followed by cardiac puncture at 8, 16, 36 or 46 weeks of age.

All mice were group-housed (3–5 animals/cage) at 20 °C with a 12h-dark/light cycle in conventional animal facilities. Mice had ad libitum access to a standard rodent diet (R/M-H; Ssniff Spezialdiäten GmbH) and to water.

Surgical procedures

A cohort of N-ARKO mice and hemizygous Thy1-CreERT2 control littermates underwent orchidectomy (ORX; abdominal approach) under isoflurane anaesthesia followed by buprenorphine analgesia (60 µg/kg SC) at 16 weeks of age. Implants of medical-grade silicone tubing (Silclear®, Degania Medical, Degania, Israel) sealed with medical adhesive silicone (Silastic®, Biesterfeld, Germany) were implanted in the nuchal region, either filled with T or DHT (both from Sigma-Aldrich, St. Louis, MO, USA). In our previous work, we calculated that the daily dose of T administered *in vivo* by 1 cm SILASTIC implant is 23 µg [21] whereas the 1.50 cm DHT SILASTIC implant has a release of 45 µg [22]. In male mice, this androgen dosage is slightly supraphysiological, as indicated by the higher seminal vesicle weight following implantation of T or DHT pellets in ORX mice compared with sham surgery group [23]. Mice with the same treatment were group-housed (3–5 animals/cage) in the same conditions as described above. Bone phenotype was determined 20 weeks post-ORX. The effectiveness of hormone replacement was demonstrated by determining the weight of the androgen-sensitive seminal vesicle and levator ani/bulbocavernosus (LA/BC) muscle complex.

Grip strength

Total-limb maximal grip strength was evaluated by means of a grid connected to an isometric force transducer (Chatillon DFIS-2 Digital Force Gauche, Ametek, Paoli, PA, USA). Mice grasping a metal grip with all limbs were pulled horizontally by their tails until they lost their grip. Measurements were registered in Newtons (N) and the result was set as the average of six attempts.

Wheel running

Animals were introduced into individual cages equipped with computerized running wheels (Linton Instrumentation Inc., Diss, Norfolk, UK). Revolutions were measured electronically in 10-min bins of activity for 19 days and afterwards the running distance was calculated [23].

Body composition

Lean and fat mass were analyzed *in vivo* using the PIXImus mouse densitometer (Lunar Corp) with an ultrahigh resolution (0.18×0.18 pixels, 1.6 line pairs/mm) and software version 1.45. In addition, individual limb muscles (gastrocnemius and soleus) were dissected *ex vivo* and wet weight measured.

Liquid chromatography- tandem mass spectrometry

Total T was measured at the University Hospitals Leuven without derivatization using a two-dimensional liquid chromatography system and an AB/Sciex QTrap 5500 tandem mass spectrometer in atmospheric pressure chemical ionization positive mode [24].

Serum analyses

Leptin (90030, Crystal Chem), noradrenaline and adrenaline (BA E-5400, LDN®, Nordhorn, Germany) levels in mouse serum were determined using commercially available kits following the manufacturers' instructions. Osteocalcin was measured using an in-house radioimmunoassay (RIA) as described previously [25]. LH and FSH were determined by ELISA and RIA, respectively, at the University of Virginia Center of Research in Reproduction Ligand Assay and Analysis Core (Charlottesville, VA).

MicroCT

Ex vivo microCT analysis on femur, tibia and L5 vertebra was performed with a SkyScan 1172 microCT (Bruker) using 5 μm pixel size, 0.5 mm Al filter, 50 kV, 200 μA, 180° angular rotation at 0.4° steps and 590 ms integration time. All images were reconstructed using NRecon and analyzed by CTAn software as described [26]. For long bones, the trabecular regions of interest started at 0.5 mm from the proximal (tibia) and distal (femur) growth plates in the direction of the metaphysis and extended for 1.5 (tibia) and 2 mm (femur). Cortical measurements were performed in the diaphyseal region starting at a distance of 0.5 mm proximally from the tibia-fibula junction or 4.5 mm proximally from the distal femoral growth plate and extending 0.25 mm. For vertebra L5, the entire trabecular bone within the vertebral body was analyzed. Parameters included trabecular bone volume fraction (BV/TV, %), trabecular number (Tb.N, 1/mm), trabecular thickness (Tb.Th, mm), trabecular separation (Tb.Sp, mm), total cross-sectional tissue area (Tt.Ar, mm^2), cortical bone area (Ct.Ar, mm^2), medullary or marrow area (Ma.Ar, mm^2), medullary area fraction (Ma. Ar/Tt. Ar, %), cortical thickness (Ct.Th, mm) and polar moment of inertia (J, mm^4). Nomenclature of all microCT data follows the guidelines of the American Society for Bone and Mineral Research (ASBMR) [27].

Bone histomorphometry

Bone formation rate (BFR) at the periosteal and endosteal surfaces of the cortical bone in the middiaphyseal region of the femur was evaluated by dynamic histomorphometric analyses. Mice were injected i.p. with calcein (15 mg/kg; Sigma-Aldrich, St. Louis, MO, USA) 12 and 1 day(s) before euthanasia. Femurs were fixed in Burckhardt's fixative (overnight, 4°C), kept in ethanol, and embedded in methyl methacrylate. Cross-sections of the undecalcified femur perpendicularly to the long axis were prepared at 200 μm thickness in the middiaphyseal region using the contact-point precision band saw (Exakt, Norderstedt, Germany). Sections were ground to a final thickness of 25 μm using a grinding system (Exakt, Norderstedt, Germany), left unstained, and subjected to dynamic histomorphometry. Three sections in the middiaphyseal region were measured by fluorescence microscopy, and the BFR (square micrometers per micrometer per day) was assessed at both the endocortical and periosteal bone surfaces. The BFR was obtained by the product of mineral apposition rate (μm/day) and mineralizing perimeter per bone perimeter (%). The mineralizing perimeter was

calculated as follows: mineralizing perimeter = [dL + (sL/2)]/bone perimeter, where dL represents the length of the double labels, and sL is the length of single labels along the entire endocortical or periosteal bone surfaces. The mineral apposition rate (µm/day) was calculated as the mean width of double labels divided by interlabel time. Osteoclast and osteoblast counts were determined in 4-µm-thick tartrate-resistant acid phosphatase (TRAcP)- and H&E-stained longitudinal sections of the femur, respectively. All images were acquired and analyzed using a Zeiss Axiovert microscope with an Axiovision (v6.1.0) image analysis system using in-house software [28,29]. All histomorphometric data are described according to ASBMR nomenclature [30].

Mechanical testing

The femora of 46-week-old N-ARKO and controls were tested in three-point bending on a Bose ElectroForce testing system (TestBench LM1, EnduraTEC Systems Group, Bose Corp., Minnetonka, MN, USA). Span length and radius of curvature of the supports were 7 mm and 2 mm, respectively. Until testing, the femora had been stored in PBS at −20°C. The bones were placed with the anterior surface pointing downward and were subjected to a small stabilizing preload (1 N) and two conditioning cycles before loading until failure at a rate of 0.1 mm/second. The following parameters were derived from the load-displacement curve: (1) ultimate bone strength (N), representing the strength of bone; (2) stiffness (N/mm), calculated as the slope of the linear portion of the load-displacement curve, representing the elastic rigidity; and (3) work-to-failure (mJ), determined as the area under the load-displacement curve, representing the energy absorbed by the bone before breaking.

Quantitative PCR

Total RNA was extracted from tissue samples by homogenization in Trizol reagent (Invitrogen, Carlsbad, CA, USA) followed by isopropanol precipitation. For cDNA synthesis, a superscript II RNaseH− reverse transcriptase kit was used (Invitrogen). The primer sequences are described in Supplemental Table 1. The PCR mixtures (10 µl) contained 5 µl Fast SYBR green Master Mix (Applied Biosystems, Foster City, CA, USA) and 0.03 µM of each primer. For quantification of gene expression, the StepOnePlus™ sequence detector PCR detection system (Applied Biosystems) was

used. All primers were designed to hybridize to different exons, and generation of single amplicons was checked in melting curve assays. The housekeeping gene hypoxanthine guanine phosphoribosyl transferase (Hprt) served as an endogenous control and expression levels were analyzed by the 2−ΔΔCT method.

Statistics

Statistical analysis was performed using Graphpad Prism v6.05. Student t-test and one- way ANOVA followed by Bonferroni's post-hoc test were used to analyze differences between two groups or more, respectively. When two independent variables were included in the analysis, two-way ANOVA was performed. All statistical tests were performed two-tailed. Data are expressed as mean ± SEM and P values < 0.05 were considered statistically significant.

Results

N-ARKO mice show normal hypothalamic-pituitary-gonadal function

We previously showed that tamoxifen administration induces the excision of floxed AR exon 2 in neural tissues of N-ARKO mice, whereas non-neural tissues, including bone, do not show CreERT2-mediated recombination [18]. Here, tamoxifen but not vehicle at 6 weeks of age resulted in a 70-80% reduction in AR expression in Thy1-CreERT2 positive brain regions cerebral cortex and brainstem ($P < 0.01$ and $P < 0.001$ *vs.* control, respectively; Fig. 1A) as well as in the peripheral nervous system, namely dorsal root ganglia ($P < 0.01$ *vs.* control; Fig. 1A) in 8-week-old mice. As expected [19], hypothalamic AR mRNA levels were only marginally affected (-20% *vs.* control; $P < 0.05$; Fig. 1A), as also confirmed at 16 weeks of age (Supplemental Fig. 1). In accordance, the HPG function seemed unaltered in N-ARKO mice, with no changes in serum T, LH or FSH levels ($P > 0.05$, Fig.1B-D). However, the weight of androgen-sensitive seminal vesicles was increased in 36- and 46 week-old N-ARKO mice [genotype: $F(1,142) = 83.51$, $P < 0.0001$; age: $F(2,142) = 85.63$, $P < 0.0001$; interaction: $F(2,142) = 10.79$, $P < 0.0001$; Fig. 1E]. To investigate whether this was due to an intrinsic genotype-dependent mechanism or secondary to an altered hormonal milieu, we determined the weight of seminal vesicles following ORX with or without hormone replacement. The differences in seminal

vesicle weight between genotypes disappeared in ORX mice receiving placebo or a fixed amount of T or DHT (Supplemental Fig. 2A), suggesting that the cause of larger seminal vesicles in N-ARKO mice was a higher peripheral androgen bioactivity, despite normal serum T.

Deletion of AR in extrahypothalamic neurons does not affect body weight or body composition

The evolution of body weight during the 9-week period after tamoxifen administration (6 weeks of age) was comparable between N-ARKO and control littermates (Supplemental Fig. 2B). In addition, body weight at 16, 36 and 46 weeks of age was indistinguishable between genotypes (Fig. 1F). Body composition, as assessed by DXA scan, was also similar between N-ARKO and control mice, regardless of age (Fig. 1G). Deletion of neuronal AR did not reproduce the decrease in muscle mass and strength observed after ORX (Table 1). The mass of hindlimb (gastrocnemius and soleus) and perineal LA/BC muscles were comparable between genotypes at 46 weeks of age (Table 1). Accordingly, N-ARKO mice performed as well as control mice in the grip strength (Table 1) and wheel running tests (Supplemental Fig. 2C).

Deletion of AR in extrahypothalamic neurons accelerates age-related loss of cortical bone

N-ARKO mice had normal femur length compared with control littermates at both 16 and 36 weeks of age (data not shown). MicroCT analysis of the femur revealed that deletion of neuronal AR did not affect the acquisition of cortical bone at 16 weeks of age (Fig. 2A-E). As expected [31], cortical thickness decreased from 16 to 36 weeks of age, but this decline was more pronounced in N-ARKO mice compared to controls [genotype: $F(1,96) = 14.19$, $P = 0.0003$; age: $F(2,96) = 24.24$, $P < 0.0001$; interaction: $F(2,96) = 3.476$, $P < 0.05$; Fig. 2B and E]. In addition, N-ARKO mice showed a loss of cortical area [genotype: $F(1,96) = 7.68$, $P < 0.01$; age: $F(2,96) = 8.22$, $P < 0.001$; interaction: $F(2,96) = 1.7$, $P > 0.05$; Fig. 2C and E] associated to an increased medullary area fraction [genotype: $F(1,96) = 7.96$, $P < 0.001$; age: $F(2,96) = 23.74$, $P < 0.0001$; interaction: $F(2,96) = 1.15$, $P > 0.05$; Fig. 2D], whilst periosteal circumference remained unaffected (data not shown). These findings were further confirmed in the tibia (Supplemental Fig. 3A-D).

To rule out the possibility that the previous observations were confounded by subtle alterations in the hormonal status of N-ARKO mice, we examined femoral cortical bone microstructure following ORX with T or DHT replacement (Table 2). In accordance to findings in gonadally intact animals, 36-week-old ORX N-ARKO mice treated with hormone replacement displayed a decline in cortical thickness and area compared to treatment-matched controls, although post hoc analysis only revealed significant differences in the setting of T, but not DHT (Table 2).

Deletion of neuronal AR did not alter the acquisition or maintenance of trabecular bone mass in the femur (Table 3). In contrast, N-ARKO mice displayed a decrease in cancellous bone volume fraction and trabecular number in L5 vertebra with aging, which reached statistical significance at 36 weeks of age [genotype: $F(1,60) = 5.69$, $P < 0.05$; age: $F(2,60) = 2.316$, $P > 0.05$; interaction: $F(2,60) = 4.382$, $P<0.05$; Table 3].

N-ARKO mice display reduced bone strength.

Mechanical properties of the femur were determined by three-point bending test. Inactivation of AR in neurons reduced maximum load and energy to failure in 46-week-old gonadally intact mice, whilst stiffness was unaffected ($P < 0.05$ and $P < 0.01$, respectively; Fig. 3A-C). The decrease in bone strength in N-ARKO mice was comparable to that observed in age-matched ORX mice, regardless of genotype (Fig. 3A-C).

Bone formation and resorption in N-ARKO mice

To determine whether the accelerated cortical thinning in N-ARKO mice was due to a decrease in bone formation and/or an increase in bone resorption, we performed histomorphometric, gene expression and biochemical analyses at 36 or 46 weeks of age. Bone apposition parameters (MS/BS, MAR, BFR) at the endocortical and periosteal surfaces of the mid-diaphyseal femur were indistinguishable between genotypes (Fig. 4A-H). Similarly, the number of osteoblasts in the femoral trabecular bone (Fig. 4K), transcription of osteoblast-related genes in the tibia and serum osteocalcin - a marker for bone formation- were not significantly altered in N-ARKO mice (Supplemental Table 2). Osteoclast-covered bone surfaces, as determined by TRAP-staining, were increased by 30% in N-

ARKO mice in the femoral trabecular but not endocortical compartment (Fig. 4I-M). Osteoclast-specific transcripts in tibia and serum CTX, a marker for bone resorption, remained unaffected (Supplemental Table 2).

We next examined whether the cortical thinning in N-ARKO mice was associated to an increased SNS outflow. The expression of the thermogenic gene *Ucp1* in brown adipose tissue (BAT), an extensively used surrogate marker of SNS peripheral outflow [32], was indistinguishable between genotypes at 16 weeks of age whereas it was up-regulated in 46-week-old N-ARKO mice compared to controls (Fig. 5A). Control mice undergoing ORX at 16 weeks of age displayed a similar but non-significant increase in *Ucp1* expression at 46 weeks compared to gonadally intact controls [genotype: $F(1,25) = 7.09$, $P=0.01$; ORX: $F(1,25) = 3.10$, $P=0.09$; interaction: $F(1,25) = 1.24$, $P > 0.05$; Fig. 5A]. However, androgen deficiency did not further increase *Ucp1* transcript levels in BAT of N-ARKO mice. Serum leptin (data not shown), serum and urine catecholamine levels as well as norepinephrine content in the tibia showed no significant differences between genotypes (Fig. 5B-F).

Discussion

The osteoanabolics effects of androgens on male bone have been extensively characterized but the target cell(s) particularly mediating their actions on cortical bone compartment remain(s) incompletely understood. Our findings reveal that AR signaling in neurons is dispensable for bone acquisition at puberty but it plays a critical role protecting cortical thickness and strength in aging. These results provide the first direct evidence that androgens act on male bone via the AR in neurons.

Androgens play a major role in the gain of bone mass during puberty [1]. Androgen actions via AR in osteoblasts inhibit bone resorption in the cancellous compartment and are essential for trabecular bone accrual during growth [5,6,33]. On the other hand, the presence of AR in murine osteoclasts is doubtful and certainly does not exert antiresorptive actions [5,7]. Regarding the cortical compartment, the full action of androgens on periosteal formation requires ERα in addition to AR signaling, as evidenced in studies using AR-ERα double-knockout male mice [34]. Intriguingly, the loss of ERα in mesenchymal progenitors leads to a delay in cortical bone accrual during puberty, suggesting that AR activation can

compensate the lack of ERα signaling in these cells [5,35]. Also in young male mice, androgen actions on neurons do not mediate the key effects of AR on periosteal formation, as shown in this study. Clearly, this stands in contrast to the well-established role of central ERα inhibiting cortical acquisition in growing females [13,36]. The striking differences between our findings and those observed in N-ERαKO female mice could be explained by the persistence of hypothalamic expression in our model. Indeed, ERα signaling in arcuate neurons was identified as the mechanism behind the central effects of E2 on female bone [14,36]. Nevertheless, N-ARKO male mice with an AR hypothalamic insensitivity showed normal whole-body BMD, as assessed by DXA scan [37]. Notwithstanding the technical limitations of the last study, these findings suggest that sex steroid actions on neurons are only determinant for bone mass acquisition in females. Overall, although our study shows a role for neuronal AR in age-related cortical thinning, the cellular targets mediating the essential effects of androgens on male pubertal periosteal bone expansion remain unknown.

Cortical thinning of long bone diaphyses starts at approximately 5.5 months of age and slowly progresses with aging in C57BL/6J male mice [31]. It therefore came as no surprise that 36- and 46-week-old-mice exhibited losses in cortical thickness and area compared to 16-week-old controls. However, inactivation of AR in neurons accelerated this age-related decay in cortical integrity as well as strength. Importantly, this was not secondary to a defect in bone accrual since cortical parameters were not affected in N-ARKO mice right after puberty. The observation that normal age-related bone loss in male mice occurred in the setting of sex steroid sufficiency, as assessed by SV weight and serum T, makes our findings even more intriguing. Previous studies already indicated that sex steroid bioactivity remains stable in elderly rodents [9,38]. Noteworthy, Ucer *et al*. [38] proved that the molecular and cellular mechanisms implicated in the loss of murine cortical bone by sex steroid deficiency and aging were independent. Thus, we conclude that a decreased androgen bioactivity is not a primary mechanism for age-related bone loss in male mice but, still, an intact neuronal AR function is required to preserve cortical integrity.

The loss of cortical bone induced by ORX is mechanistically different in growing and non-growing rodents [39]. Androgen deficiency blunts periosteal expansion at peripubertal ages [40] whilst an

increased endocortical resorption is the main cause of cortical loss following ORX in adulthood [39]. Similarly, cortical thinning in 36- and 46-week-old N-ARKO mice was secondary to an augmented endocortical expansion (Fig.2).

Neuronal AR deletion reduced the trabecular bone volume fraction in the axial but not appendicular skeleton of N-ARKO mice with aging. The available evidence so far indicates that osteoblasts are the main target cells for the stimulatory effects of AR on trabecular bone compartment [4]. Our data extend the current understanding by showing that neurons also contribute to AR-protective effects on trabecular bone mass in male axial skeleton with aging.

The negative feedback regulation of serum sex steroids was profoundly disturbed in previous models of hypothalamic AR [37,41] and ERα [14,42] inactivations in male and female mice, respectively. In this study, N-ARKO generated using Thy1-CreERT2 displayed normal levels of serum T, LH and FSH. In agreement, wheel running activity, which we have previously established as a sensitive marker of androgen activity [23,43], remained unaltered following AR inactivation in neurons. However, seminal vesicle weight, a frequently used readout for androgen levels [24], was increased in N-ARKO mice, despite less than in previous N-ARKO mouse models with a complete neuronal AR inactivation in the hypothalamus [41]. Since seminal vesicle weight might be more sensitive than serum T reflecting changes in androgen activity in male rodents [44], we determined the bone phenotype of N-ARKO mice following ORX and hormone replacement in order to rule out potential confounding from subtle alterations in sex steroid levels. N-ARKO mice receiving a fixed amount of T displayed a similar accelerated cortical thinning to that observed in gonadally intact animals, demonstrating that a disturbed HPG axis was not interfering with our observations. In fact, a slightly higher circulating androgen bioactivity in N-ARKO mice would be expected to maintain rather than accelerate cortical bone loss as shown here.

A growing body of evidence supports a role for SNS acting as a downstream mechanism whereby CNS neurons regulate the activity of bone cells [12,16,45]. Stimulation of beta 2 adrenergic receptor (*Adrb2*) in osteoblasts following sympathetic activation reduces bone formation and increases resorption via stimulation of *Rankl* [16]. *Ucp1* expression in BAT was the only marker of SNS activity

increased in N-ARKO mice. However, we cannot exclude the possibility that *Ucp1* increase took place once the bone phenotype was established and/or that it was secondary to non-SNS signals. Thus, unfortunately, our data does not allow us to determine conclusively the implication of the SNS in the observed changes in bone.

Bone homeostasis is influenced by muscle-bone interactions [46]. It is unclear if androgens may have indirect effects on bone mass by stimulating muscle mass and strength [3]. We recently showed that AR deletion in the myogenic lineage [47] accelerated age-related trabecular bone loss but did not influence cortical bone or the severity of trabecular disuse osteopenia in male mice [3]. Here, inactivation of AR in neurons did not recapitulate the detrimental effects of androgen deficiency on hindlimb muscle mass, grip strength and wheel running activity, thus excluding the possibility that the bone phenotype of N-ARKO mice was secondary to a loss of muscle function. Our results differ from those obtained by Davey *et al.* [41] showing that AR signaling in brain, including hypothalamic regions, positively regulates hind-limb muscle mass. Whether differences between studies reflect a role for hypothalamic AR remains to be determined.

The term extrahypothalamic is used here to differentiate our N-ARKO mice from prior N-ARKO models showing a profound disturbance of the HPG axis [37,41], even though we acknowledge that this is a simplified view since we observed a marginal but significant decrease in hypothalamic AR expression. Be that as it may, hypothalamic AR might still play a role modulating the peripheral effects of androgens on trabecular bone. Finally, due to the complexity of characterizing slow imbalances in endocortical remodeling, we could not conclude whether the accelerated cortical thinning in N-ARKO mice was secondary to a decreased formation or an increased resorption [39].

In conclusion, our study highlights that neuronal AR exerts age- and compartment-specific actions on male bone. In particular, we showed that androgen signaling through AR expressed in neurons protects cortical bone from age-related involution, restraining the loss of cortical thickness due to medullary expansion. Further studies are warranted to identify the specific pool of AR-positive neurons implicated in the observed effects.

Acknowledgments

We thank Ivo Jans, Erik Vanherck, Karen Moermans and Riet Van Looveren for their excellent technical assistance and Vanessa Dubois and Kenneth Korach for their helpful discussions related to this work.

Authors' roles

Study design: FJ, ML, BD, GC, FC, and DV. Study conduct: FJ, LD, DS, HL and NK. Data collection: FJ, LD, DS, RK and NK. Data analysis: FJ. Data interpretation: FJ, ML, BD, GC, FC, and DV. Drafting manuscript: FJ. Revising manuscript content: all authors. Approving final version of manuscript: all authors. FJ takes responsibility for the integrity of the data analysis.

References

1. Vanderschueren D, Laurent MR, Claessens F, Gielen E, Lagerquist MK, Vandenput L, et al. Sex steroid actions in male bone. Endocr. Rev. 2014. p. 906–60.

2. Behre HM, Kliesch S, Leifke E, Link TM, Nieschlag E. Long-term effect of testosterone therapy on bone mineral density in hypogonadal men. J. Clin. Endocrinol. Metab. 1997;82(8):2386–90.

3. Laurent MR, Jardí F, Dubois V, Schollaert D, Khalil R, Gielen E, et al. Androgens have antiresorptive effects on trabecular disuse osteopenia independent from muscle atrophy. Bone. 2016;93:33–42.

4. Almeida M, Laurent MR, Dubois V, Claessens F, O'Brien CA, Bouillon R, et al. Estrogens and Androgens in Skeletal Physiology and Pathophysiology. Physiol. Rev. 2017;97(1):135–87.

5. Ucer S, Iyer S, Bartell SM, Martin-Millan M, Han L, Kim HN, et al. The Effects of Androgens on Murine Cortical Bone Do Not Require AR or ERα Signaling in Osteoblasts and Osteoclasts. J. Bone Miner. Res. 2015;30(7):1138–49.

6. Notini AJ, McManus JF, Moore A, Bouxsein M, Jimenez M, Chiu WSM, et al. Osteoblast deletion of exon 3 of the androgen receptor gene results in trabecular bone loss in adult male mice. J. Bone Miner. Res. 2007;22(3):347–56.

7. Sinnesael M, Jardi F, Deboel L, Laurent MR, Dubois V, Zajac JD, et al. The androgen receptor has no direct antiresorptive actions in mouse osteoclasts. Mol. Cell. Endocrinol. 2015;411:198–206.

8. Riggs BL, Melton LJ, Robb RA, Camp JJ, Atkinson EJ, McDaniel L, et al. A population-based assessment of rates of bone loss at multiple skeletal sites: Evidence for substantial trabecular bone loss in young adult women and men. J. Bone Miner. Res. 2008;23(2):205–14.

9. Hamrick MW, Ding K-H, Pennington C, Chao YJ, Wu Y-D, Howard B, et al. Age-related loss of muscle mass and bone strength in mice is associated with a decline in physical activity and serum leptin. Bone. 2006;39(4):845–53.

10. Sinnesael M, Claessens F, Laurent M, Dubois V, Boonen S, Deboel L, et al. Androgen receptor (AR) in osteocytes is important for the maintenance of male skeletal integrity: Evidence from targeted AR disruption in mouse osteocytes. J. Bone Miner. Res. 2012;27(12):2535–43.

11. Ducy P, Amling M, Takeda S, Priemel M, Schilling a F, Beil FT, et al Leptin inhibits bone formation through a hypothalamic relay: a central control of bone mass. Cell. 2000;100(2):197–207.

12. Takeda S, Elefteriou F, Levasseur R, Liu X, Zhao L, Parker KL, et al. Leptin regulates bone formation via the sympathetic nervous system. Cell. 2002;111(3):305–17.

13. Ohlsson C, Engdahl C, Börjesson AE, Windahl SH, Studer E, Westberg L, et al. Estrogen receptor-α expression in neuronal cells affects bone mass. Proc. Natl. Acad. Sci. U. S. A. 2012;109(3):983–8.

14. Farman HH, Windahl SH, Westberg L, Isaksson H, Egecioglu E, Schele E, et al. Female mice lacking estrogen receptor-α in hypothalamic proopiomelanocortin (POMC) neurons display

enhanced estrogenic response on cortical bone mass. Endocrinology. 2016;157(8):3242–52.

15. Khajuria DK, Razdan R, Mahapatra DR, Bhat MR. Osteoprotective effect of propranolol in ovariectomized rats: A comparison with zoledronic acid and alfacalcidol. J. Orthop. Sci. 2013;18(5):832–42.

16. Elefteriou F, Ahn JD, Takeda S, Starbuck M, Yang X, Liu X, et al. Leptin regulation of bone resorption by the sympathetic nervous system and CART. Nature. 2005;434(7032):514–20.

17. Dénes Á, Boldogkoi Z, Uhereczky G, Hornyák Á, Rusvai M, Palkovits M, et al. Central autonomic control of the bone marrow: Multisynaptic tract tracing by recombinant pseudorabies virus. Neuroscience. 2005;134(3):947–63.

18. Jardí F, Laurent MR, Dubois V, Khalil R, Deboel L, Schollaert D, et al. A shortened tamoxifen induction scheme to induce CreER recombinase without side effects on the male mouse skeleton. Mol. Cell. Endocrinol. 2017;452:57–63.

19. Young P, Qiu L, Wang D, Zhao S, Gross J, Feng G. Single-neuron labeling with inducible Cre-mediated knockout in transgenic mice. Nat. Neurosci. 2008;11(6):721–8.

20. De Gendt K, Swinnen J V., Saunders PTK, Schoonjans L, Dewerchin M, Devos A, et al. A Sertoli cell-selective knockout of the androgen receptor causes spermatogenic arrest in meiosis. Proc. Natl. Acad. Sci. 2004;101(5):1327–32.

21. Vanderschueren D, Vandenput L, Boonen S, Van Herck E, Swinnen J V., Bouillon R. An aged rat model of partial androgen deficiency: Prevention of both loss of bone and lean body mass by low-dose androgen replacement. Endocrinology. 2000;141(5):1642–7.

22. Vandenput L, Boonen S, Van HE, Swinnen J V, Bouillon R, Vanderschueren D. Evidence from the aged orchidectomized male rat model that 17beta-estradiol is a more effective bone-sparing and anabolic agent than 5alpha-dihydrotestosterone. J Bone Min. Res. 2002;17(11):2080–6.

23. Jardi F, Laurent MR, Kim N, Khalil R, De Bundel D, Van Eeckhaut A, et al. Testosterone boosts physical activity in male mice via dopaminergic pathways. Sci. Rep. 2018;8(1):957.

24. Laurent MR, Hammond GL, Blokland M, Jardí F, Antonio L, Dubois V, et al. Sex hormone-binding globulin regulation of androgen bioactivity in vivo: validation of the free hormone hypothesis. Sci. Rep. 2016;6(1):35539.

25. Verhaeghe J, Van Herck E, Van Bree R, Van Assche FA, Bouillon R. Osteocalcin during the reproductive cycle in normal and diabetic rats. J. Endocrinol. 1989;120(1).

26. Laperre K, Depypere M, van Gastel N, Torrekens S, Moermans K, Bogaerts R, et al. Development of micro-CT protocols for in vivo follow-up of mouse bone architecture without major radiation side effects. Bone. 2011;49(4):613–22.

27. Bouxsein ML, Boyd SK, Christiansen BA, Guldberg RE, Jepsen KJ, Müller R. Guidelines for assessment of bone microstructure in rodents using micro-computed tomography. J. Bone Miner. Res. 2010. p. 1468–86.

28. Sinnesael M, Laurent MR, Jardi F, Dubois V, Deboel L, Delisser P, et al. Androgens inhibit the osteogenic response to mechanical loading in adult male mice. Endocrinology. 2015;156(4):1343–53.

29. Masuyama R, Stockmans I, Torrekens S, Van Looveren R, Maes C, Carmeliet P, et al. Vitamin D receptor in chondrocytes promotes osteoclastogenesis and regulates FGF23 production in osteoblasts. J. Clin. Invest. 2006;116(12):3150–9.

30. Dempster DW, Compston JE, Drezner MK, Glorieux FH, Kanis JA, Malluche H, et al. Standardized nomenclature, symbols, and units for bone histomorphometry: A 2012 update of the report of the ASBMR Histomorphometry Nomenclature Committee. J. Bone Miner. Res. 2013. p. 2–17.

31. Halloran BP, Ferguson VL, Simske SJ, Burghardt A, Venton LL, Majumdar S. Changes in bone structure and mass with advancing age in the male C57BL/6J mouse. J. Bone Miner. Res. 2002;17(6):1044–50.

32. Virtue S, Vidal-Puig A. Assessment of brown adipose tissue function. Front. Physiol. 2013;4.

33. Russell PK, Clarke M V., Cheong K, Anderson PH, Morris HA, Wiren KM, et al. Androgen receptor action in osteoblasts in male mice is dependent on their stage of maturation. J. Bone Miner. Res. 2015;30(5):809–23.

34. Callewaert F, Venken K, Ophoff J, De Gendt K, Torcasio A, van Lenthe GH, et al. Differential regulation of bone and body composition in male mice with combined inactivation of androgen and estrogen receptor-alpha. FASEB J. 2009;23(1):232–40.

35. Almeida M, Iyer S, Martin-Millan M, Bartell SM, Han L, Ambrogini E, et al. Estrogen receptor-α signaling in osteoblast progenitors stimulates cortical bone accrual. J. Clin. Invest. 2013;123(1):394–404.

36. Herber C, Krause W, Cain C, Wang L, Hsiao E, Nissenson1 R, et al. Disrupting Central Estrogen Receptor a Signaling in the Arcuate Nucleus Produces a Dramatic Increase in Bone Mass and Strength. J Bone Min. Res. 2007;32(S1):S27.

37. Raskin K, de Gendt K, Duittoz A, Liere P, Verhoeven G, Tronche F, et al. Conditional Inactivation of Androgen Receptor Gene in the Nervous System: Effects on Male Behavioral and Neuroendocrine Responses. J. Neurosci. [Internet]. 2009;29(14):4461–70. Available from: http://www.jneurosci.org/cgi/doi/10.1523/JNEUROSCI.0296-09.2009

38. Ucer S, Iyer S, Kim HN, Han L, Rutlen C, Allison K, et al. The Effects of Aging and Sex Steroid Deficiency on the Murine Skeleton Are Independent and Mechanistically Distinct. J. Bone Miner. Res. 2017;32(3):560–74.

39. Reim NS, Breig B, Stahr K, Eberle J, Hoeflich A, Wolf E, et al. Cortical bone loss in androgen-deficient aged male rats is mainly caused by increased endocortical bone remodeling. J. Bone Miner. Res. 2008;23(5):694–704.

40. Ke HZ, Crawford DT, Qi H, Chidsey-Frink KL, Simmons H a, Li M, et al. Long-term effects of aging and orchidectomy on bone and body composition in rapidly growing male rats. J. Musculoskelet. neuronal Interact. 2001;1(3):215–24.

41. Davey RA, Clarke M V., Russell PK, Rana K, Seto J, Roeszler KN, et al. Androgen action via the androgen receptor in neurons within the brain positively regulates muscle mass in male mice. Endocrinology. 2017;158(10):3684–95.

42. Xu Y, Nedungadi TP, Zhu L, Sobhani N, Irani BG, Davis KE, et al. Distinct hypothalamic neurons mediate estrogenic effects on energy homeostasis and reproduction. Cell Metab. 2011;14(4):453–65.

43. Jardí F, Laurent MR, Dubois V, Kim N, Khalil R, Decallonne B, et al. Androgen and estrogen actions on male physical activity: A story beyond muscle. J. Endocrinol. 2018. p. R31–52.

44. Coquelin A, Desjardins C. Luteinizing hormone and testosterone secretion in young and old male mice. Am. J. Physiol. 1982;243:E257–63.

45. Vignaux G, Ndong JDLC, Perrien DS, Elefteriou F. Inner ear vestibular signals regulate bone remodeling via the sympathetic nervous system. J. Bone Miner. Res. 2015;30(6):1103–11.

46. Laurent MR, Dubois V, Claessens F, Verschueren SMP, Vanderschueren D, Gielen E, et al. Muscle-bone interactions: From experimental models to the clinic? A critical update. Mol. Cell. Endocrinol. 2016;432:14–36.

47. Dubois V, Laurent MR, Sinnesael M, Cielen N, Helsen C, Clinckemalie L, et al. A satellite cell-specific knockout of the androgen receptor reveals myostatin as a direct androgen target in skeletal muscle. FASEB J. 2014;28(7):2979–94.

Figure legends

Fig. 1. Neuronal inactivation of AR in extrahypothalamic brain regions does not disturb the normal hypothalamic-pituitary-gonadal axis. (A) AR mRNA levels in hypothalamus, cerebral cortex, brainstem and dorsal root ganglia in 8-week-old mice (n=4-9/group). (B) Serum testosterone in 16- and 36-week-old mice (n=9-11/group). (C) LH (D) and FSH levels in 46-week-old mice (n=12-13/group). Longitudinal evolution of (E) seminal vesicle and (F) body weights (n=12-53/group). (G) Percentage of lean and fat mass by DXA (n=10-38/group). Data in panels B-D were analyzed using Student t-test and those in panels A and E–F were analyzed by one and two-way ANOVA with Bonferroni correction, respectively. Data are mean ± SEM. *, **, ***, **** $P < 0.05$, 0.01, 0.001, 0.0001 *vs.* age-matched controls. BS brainstem, CTX cerebral cortex, DRG dorsal root ganglia, HYP hypothalamus, SV seminal vesicles.

Fig. 2. N-ARKO display an accelerated age-related cortical thinning. (A-D) Cortical bone measurement in the midshaft femur (n=6-49/group). (E) Representative 3D models of cortical regions of interest. Data were analyzed using two-way ANOVA with Bonferroni correction. Data are mean ± SEM. **, **** $P < 0.01$, 0.0001 *vs.* age-matched controls; # $P=0.05$ *vs.* age-matched controls. a,b $P < 0.05$ *vs.* genotype-matched 16-week-old mice. c $P < 0.05$ *vs.* genotype-matched 36-week-old mice.

Fig. 3. Inactivation of neuronal AR decreases bone strength with aging (A-D) Mechanical properties (three-point bending test) of femur in gonadally intact and ORX 46-week-old mice (n=5-12/group). Data were analyzed using two-way ANOVA with Bonferroni correction. Data are mean ± SEM. *,** $P < 0.05$, 0.01 *vs.* controls. A < 0.05 *vs.* genotype-matched gonadally intact controls.

Fig. 4. Effects of neuronal AR inactivation on bone formation and resorption. Representative fluorescent micrographs of midshaft femur sections showing calcein double labels (Ps.S, periosteal surface; Ec.S, endocortical surface; scale bar, 100 μm) in (A) control and (B) N-ARKO mice. (C,F) Mineralizing surface per bone surface, (D,G) mineral apposition rate and (E, H) bone formation rate in (C-E) periosteal and (F-H) endocortical surfaces of the midshaft femur in 46-week-old mice

(n=10/group). Representative microphotographs of TRAcP staining of femoral trabecular bone of (I) control and (J) N-ARKO mice (scale bar, 100 μm). Number of osteoblasts per bone surface (K) and osteoclast surface per (L) trabecular and (M) endocortical surface in the femur of 36-week-old mice (n=6/group). Data are mean ± SEM. ** $P < 0.01$ *vs.* controls.

Fig. 5. Cortical bone loss in N-ARKO mice is associated with an increased *Ucp1* expression in brown adipose tissue. (A) *Ucp1* mRNA levels in brown adipose tissue (n=5-11/group). (B,C) Serum, (D,E) urine and (F) bone levels of (B,D) epinephrine and (C,E,F) norepinephrine in 46-week-old mice (n=7-13/group). Data are mean ± SEM. * $P < 0.05$ *vs.* controls.

Table 1. Muscle parameters of 46-week-old N-ARKO mice

	Gonadally intact		ORX	
	control (n=13)	N-ARKO n=12)	control (n=5)	N-ARKO (n=6)
Skeletal mass (mg)				
LA/BC	93.5±3.36	95.13±2.73	16.63±1.69****	15.74±2.51****
GASTR	136.3±2.81	134.9±2.31	118.4±3.84**	114.1±3.11***
SOL	7.69±0.29	7.12±0.42	7±0.53	8±1.28
Grip strength (N)	3.06±0.1	2.94±0.05	2.55±0.1**	2.7±0.05

Data are mean ± SEM. **, ***, **** P < 0.01, 0.001, 0.0001 *vs.* gonadally intact genotype-matched controls. GASTR gastrocnemius, LA/BC levator ani/bulbocavernosus, SOL soleus.

Table 2. Cortical bone measurements in the midshaft femur of 36-week-old ORX+T/DHT-treated mice

	ORX+T		ORX+DHT	
	control (n=13)	N-ARKO n=15)	control (n=13)	N-ARKO (n=11)
Tt. Ar (mm^2)	2.051±0.07	1.928±0.06	1.859±0.06	1.851±0.04
Ct. Th (mm)	0.1801	0.1661**	0.1572	0.151
Ct. Ar (mm^2)	0.8442±0.03	0.757±0.02**	0.702±0.01	0.678±0.01
Ma. Ar/Tt. Ar	0.587	0.605	0.620	0.6328

Data are mean ± SEM. ** P < 0.01 vs. treatment-matched controls. DHT dihydrotestosterone, T testosterone.

	control			**N-ARKO**		
	16 weeks (n=8-13)	36 weeks (n=13-48)	46 weeks (n=13)	16 weeks (n=6-8)	36 weeks (n=10-13)	46 weeks (n=12)
Femur						
BV/TV (%)	15.19±0.48	12.49±0.39 [a]	11.14±0.52 [b]	16.28±1.04	10.7±0.35 [a]	10.08±0.48 [b]
Tb. N (1/mm)	3.71±0.08	2.66±0.06 [a]	2.4±0.11 [b]	3.8±0.28	2.43±0.08 [a]	2.27±0.1 [b]
Tb. Th (mm)	0.041±0.001	0.048±0.0005 [a]	0.046±0.0009 [b]	0.043±0.0009	0.044±0.0007**	0.044±0.0006
Tb. Sp (mm)	0.18±0.002	0.22±0.003 [a]	0.23±0.005 [b]	0.17±0.009	0.22±0.003 [a]	0.238±0.005 [b]
L5 vertebra						
BV/TV (%)	18.36±0.72	19.08±0.85	18.17±0.76	18.74±0.67	15.39±0.47**	16.73±0.44
Tb. N (1/mm)	5.46±0.16	5.71±0.19	4.93±0.18 [c]	5.59±0.12	4.95±0.09** [a]	4.69±0.13 [b]
Tb. Th (mm)	0.034±0.0013	0.033±0.0006	0.037±0.0015 [c]	0.034±0.0009	0.031±0.0006	0.036±0.0012 [c]
Tb. Sp (mm)	0.16±0.004	0.17±0.004	0.17±0.005	0.16±0.006	0.18±0.003	0.18±0.003 [b]

Table 3. Trabecular bone measurements in the distal femoral metaphysis and L5 vertebra

Data are mean ± SEM. ** P < 0.01 *vs.* age-matched controls. a,b P < 0.05 *vs.* genotype-matched 16-week-old mice. c P < 0.05 *vs.* genotype-matched 36-week-old mice.

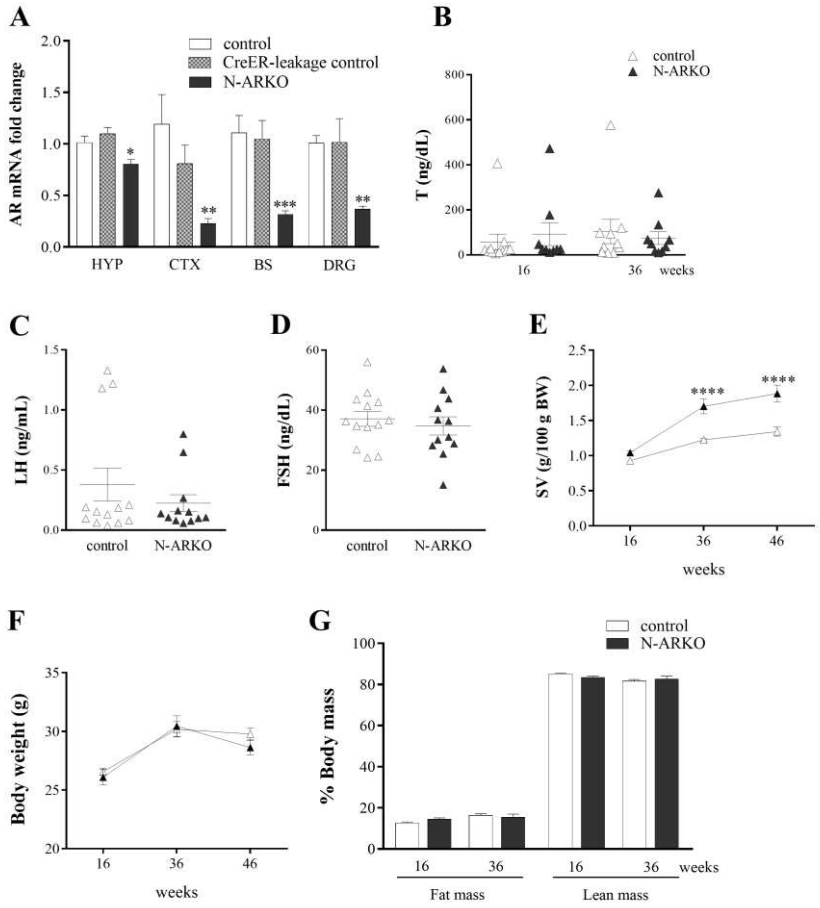

Figure 1

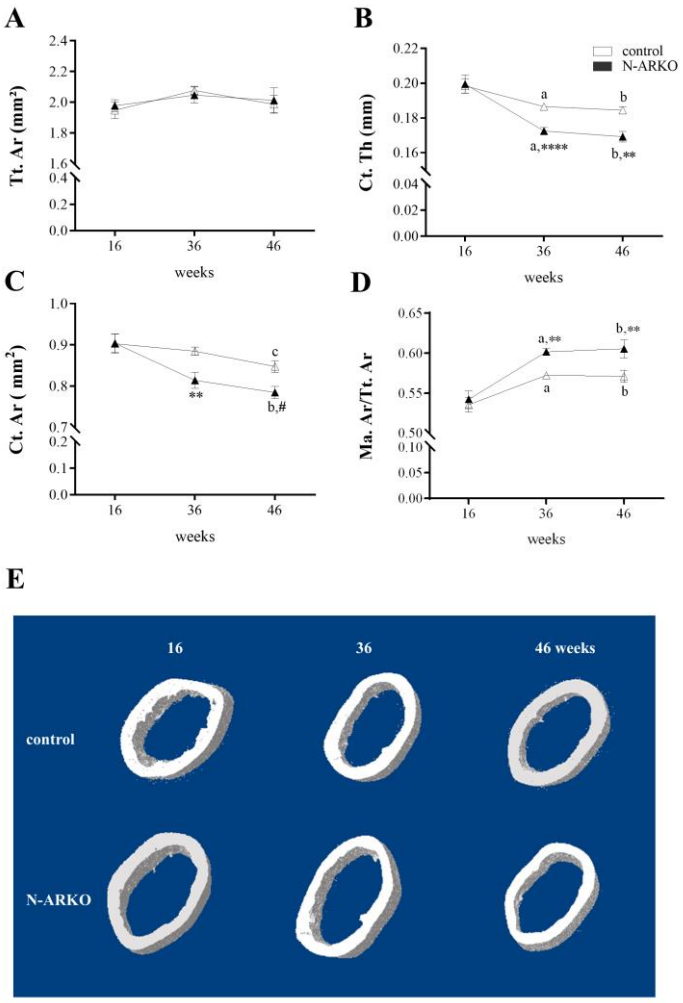

Figure 2

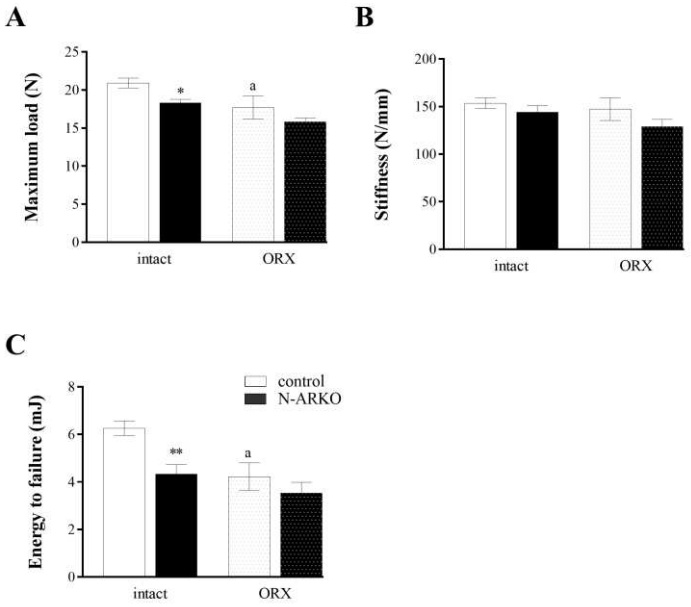

Figure 3

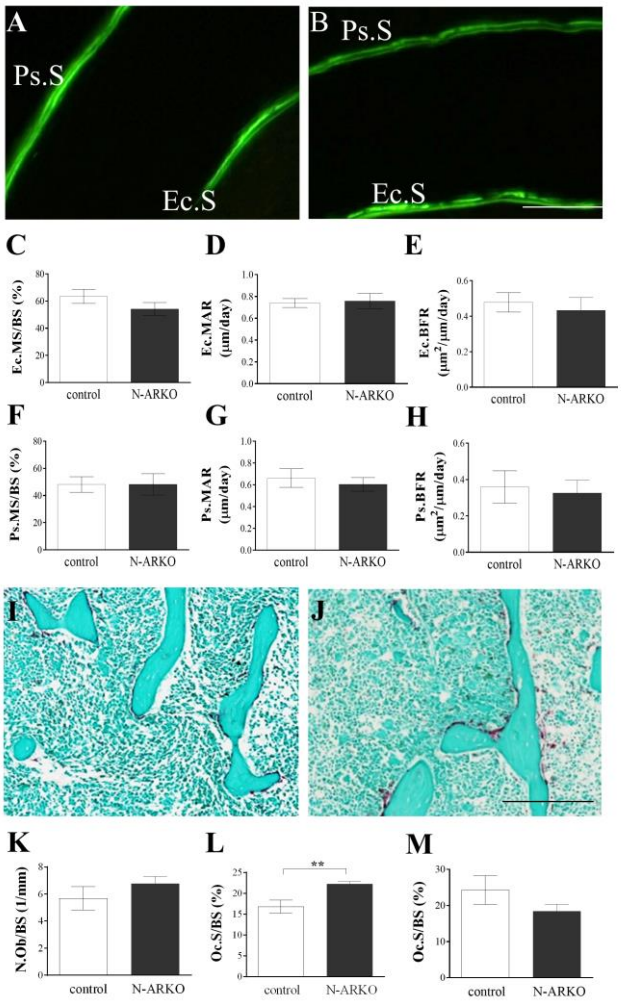

Figure 4

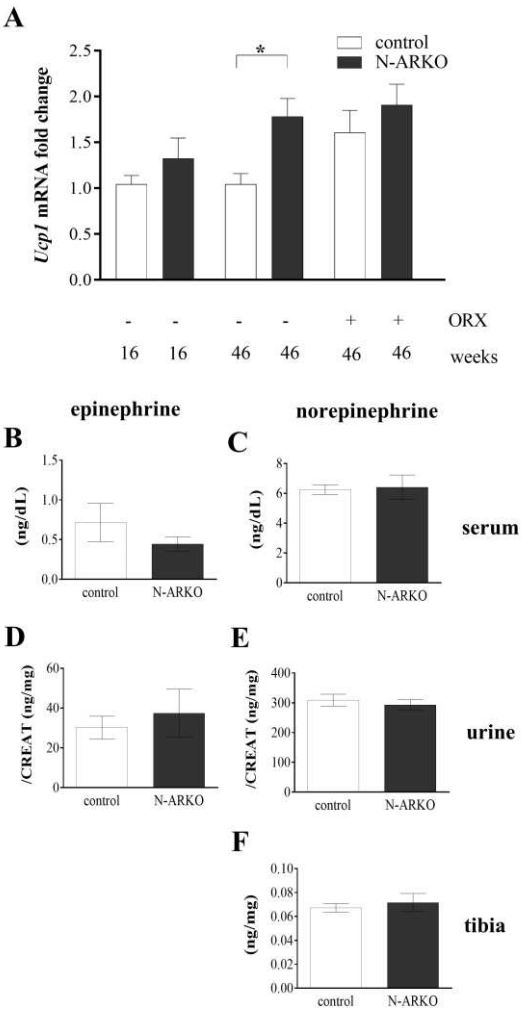

Figure 5